Chinese Chemical Letters 33 (2022) 1889–1894

Contents lists available at ScienceDirect

Chinese Chemical Letters

journal homepage: www.elsevier.com/locate/cclet

The complexation of insulin with sodium *N*-[8-(2-hydroxybenzoyl)amino]-caprylate for enhanced oral delivery: Effects of concentration, ratio, and pH

Huixian Weng[a,b,1], Lefei Hu[c,1], Lei Hu[b,d], Yihan Zhou[a,b], Aohua Wang[b,e], Ning Wang[b,e], Wenzhe Li[b,e], Chunliu Zhu[b], Shiyan Guo[b], Miaorong Yu[b], Yong Gan[a,b,e,f,*]

[a] *School of Chinese Materia Medica, Nanjing University of Chinese Medicine, Nanjing 210046, China*
[b] *State Key Laboratory of Drug Research, Shanghai Institute of Materia Medica, Chinese Academy of Sciences, Shanghai 201203, China*
[c] *School of Pharmacy, Nanjing University of Chinese Medicine, Nanjing 210023, China*
[d] *Nano Science and Technology Institute, University of Science and Technology of China, Nanjing 215123, China*
[e] *University of Chinese Academy of Sciences, Beijing 100049, China*
[f] *NMPA Key Laboratory for Quality Research and Evaluation of Pharmaceutical Excipients, National Institutes for Food and Drug Control, Beijing 100050, China*

ARTICLE INFO

Article history:
Received 27 July 2021
Revised 29 September 2021
Accepted 11 October 2021
Available online 16 October 2021

Keywords:
Oral insulin delivery
Permeation enhancer
SNAC
Absorption mechanism
Molecular interaction

ABSTRACT

Permeation enhancers (PEs), such as *N*-[8-(2-hydroxybenzoyl)amino]-caprylate (SNAC), have been reported to improve the oral absorption of various macromolecules. However, the bioavailabilities of these formulations are quite low and variable due to the influences of enzymes, pH and other gastrointestinal barriers. In this study, we revealed that SNAC could interact with insulin to form tight complexes in a specific concentration (insulin ≥ 40 μg/mL)-, ratio (SNAC/insulin ≥ 20:1)- and pH (≥ 6.8)-dependent manner, thus contributing to a significantly high efficacy of oral insulin delivery. Specifically, absorption mechanism studies revealed that the SNAC/insulin complexes were internalized into the cells by passive diffusion and remained intact when transported in the cytosol. Furthermore, the complexes accelerated the exocytosis of insulin to the basolateral side, thereby enhancing its intestinal mucosal permeability. Eudragit® S100-entrapped SNAC/insulin microspheres were then prepared and exhibited an apparent permeability coefficient (P_{app}) that was 6.6-fold higher than that of the insulin solution. In diabetic rats, hypoglycemic activity was sustained for more than 10 h after the microspheres were loaded into enteric-coated capsules. Further pharmacokinetic studies revealed an approximately 6.3% oral bioavailability in both the fasted and fed states, indicating a negligible food effect. Collectively, this study provides insight into the interaction between PEs and payloads and presents an SNAC-based oral insulin delivery system that has high oral bioavailability and patient-friendly medication guidance.

Oral delivery of macromolecules, such as proteins, peptides and RNA, has long been pursued due to its enhanced patient compliance and convenience [1]. However, due to their physicochemical characteristics and the existence of gastrointestinal barriers, the oral bioavailability of macromolecules is generally low [2,3]. In recent decades, numerous strategies, including drug modification, formulation optimization and nanoparticle-based delivery systems, have been developed to address this challenge [4–6]. One promising approach is to coformulate macromolecules with permeation enhancers (PEs) [7–10]. At present, more than 50 clinical trials have shown that PEs, such as medium-chain fatty acids, acyl carnitines, bile salts and ethylenediaminetetraacetic acid (EDTA), can increase the oral absorption of poorly permeable macromolecules, including insulin, glucagon-like peptide-1 (GLP-1) and octreotide. However, although two oral peptide formulations based on PEs, *i.e.*, semaglutide (Rybelsus®, Novo Nordisk, Denmark) and octreotide (Mycapssa®, Chiasma, Israel), are successfully marketed, their oral bioavailability is still limited (~1%) and variable [9,11]. Therefore, strategies to improve the performance of PEs are still needed.

Sodium *N*-[8-(2-hydroxybenzoyl)amino]-caprylate (SNAC), the most extensively studied PE, is now approved for the oral delivery of semaglutide [9]. Compared to the mechanism of opening tight junctions of the other PEs, SNAC improve transcellular permeation by changing the solubility of semaglutide and/or affecting

* Corresponding author.
E-mail address: ygan@simm.ac.cn (Y. Gan).
[1] These authors contributed equally to this work.

https://doi.org/10.1016/j.cclet.2021.10.023
1001-8417/

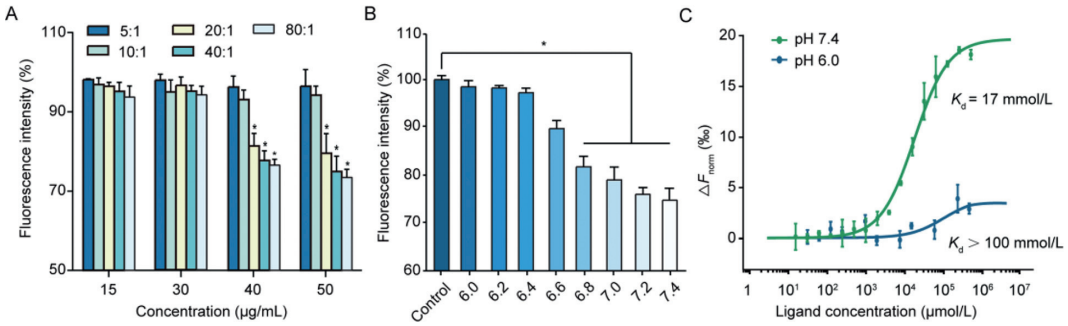

Fig. 1. (A) Fluorescence intensity changes in the SNAC and FITC-Ins physical mixture solution at different FITC-Ins concentrations (15, 30, 40 and 50 μg/mL) and different SNAC:FITC-Ins mass ratios (5:1, 10:1, 20:1 and 40:1, mean ± SD, $n = 3$). $^*P < 0.05$, compared with free FITC-Ins solution without SNAC. (B) Fluorescence intensity reductions in the SNAC and FITC-Ins (50 μg/mL, SNAC:FITC-Ins = 20:1) physical mixture solution at different pH values (mean ± SD, $n = 3$). $^*P < 0.05$, compared with FITC-Ins dissolved in HBSS at different pH values (6.0–7.4). (C) MST analysis of SNAC binding to insulin under different pH conditions.

the perturbation/fluidization of the cell membrane [12–14], thus exhibiting good biosafety [15–17]. However, Rybelsus® has a relatively low bioavailability of approximately 1%, leading to the need for high doses of semaglutide (7 or 14 mg) and SNAC (300 mg). In addition, dynamic and complex gastrointestinal conditions, such as gastrointestinal transit, fluid volume, and gastrointestinal fluid composition, reduce the concentration of SNAC needed for permeation enhancement, resulting in complicated medication guidance and large individual differences [11]. As recent studies are focusing the optimization of PE performance in a dynamic gastrointestinal environment, there is a continuous and urgent need to clarify the mode of action of PEs. More importantly, the process of intracellular trafficking and the basolateral release of PEs and payloads have yet to be characterized to better understand the absorption mechanism.

In this study, we found that SNAC could interact with insulin in a pH-, concentration- and ratio-dependent manner. When the concentration of insulin was higher than 40 μg/mL, the mass ratio of SNAC-to-insulin was larger than 20:1 and the pH was above 6.8, SNAC formed a complex with insulin, thereby significantly enhancing the cellular internalization of insulin. Based on this finding, rationally designed SNAC and insulin coencapsulated microspheres were prepared using ultrasonic spray freeze-drying technology. In diabetic rats, microsphere-loaded Eudragit® S100-coated capsules exhibited approximately 6.3% oral bioavailability in both the fasted state and fed state. The pharmacological availability of the capsule was 13.2% in the fasted state and 13.3% in the fed state. In conclusion, we successfully designed an oral delivery system that requires low PE doses and has patient-friendly medication guidance, which might pave the way for the rational design of oral macromolecule formulations.

The FITC-labeled insulin solution (FITC-Ins) at different concentrations was incubated with an equal volume of SNAC solution (pH 7.4) at mass SNAC: FITC-Ins ratios of 5:1, 10:1, 20:1, 40:1 and 80:1. The fluorescence intensity of the FITC solution was not reduced in the presence of insulin and SNAC (Fig. S1 in Supporting information), indicating that SNAC and insulin do not directly affect the FITC molecules. However, the fluorescence intensity of the FITC-Ins and SNAC mixture was reduced significantly at the appropriate ratio and concentration. When the concentration of FITC-Ins was above 40 μg/mL and the ratio of SNAC to FITC-Ins was higher than 20:1, the fluorescence intensity of FITC-Ins was dramatically decreased (Fig. 1A). These results suggested a weak interaction between SNAC and insulin, which might have changed the environment around the FITC molecule, resulting in fluorescence intensity changes.

We then investigated the effect of pH on the fluorescence intensity of the system at a specific concentration of FITC-Ins (50 μg/mL) and a specific SNAC-to-insulin ratio (20:1). Fig. 1B shows that the fluorescence intensity significantly decreased to 82% of the initial value when the pH reached 6.8 and dropped to the lowest value at a pH of 7.4. SNAC is a weak acid (pK_a 5.08), and its carboxyl group mostly existed in the form of carboxyl groups (-COO-) as the pH increased, which was conducive to the formation of a 'complex' between -COO- and the free amino group of insulin. The formation of the 'complex' changed the microenvironment around the FITC molecule attached to the phenylalanine amino group in insulin, thus affecting the fluorescence intensity of FITC-Ins.

These results indicated that SNAC interacted with insulin in the simulated intestinal medium at a pH ranging from 6.8 to 7.4. Based on these results, we propose that the interaction between SNAC and insulin is concentration-, ratio- and pH-dependent.

Microscale thermophoresis (MST) was used to detect the affinity between insulin and SNAC. As shown in Fig. 1C, the dissociation constant K_d of SNAC binding to insulin was 17 mmol/L at pH 7.4 and was larger than 100 mmol/L at pH 6.0, indicating that a weak interaction indeed existed between SNAC and insulin, and that this interaction was pH dependent. The infrared spectra of the physical mixture solution were also determined. As shown in Fig. S2 (Supporting information), the characteristic peak of SNAC at 3479 cm^{-1} (O–H stretch) moved to 3365 cm^{-1}, and the peak shape became wider, indicating potential intermolecular hydrogen bonds between insulin and SNAC.

Further, the mechanism of SNAC and insulin forming the complex under certain conditions could be explained as follows: (1) A sufficient molar ratio and a suitable pH must be required to ensure the interactions between insulin and SNAC such as hydrogen bonds; (2) an appropriate concentration ensured the sufficient frequency of collisions between insulin and SNAC which could accelerate the formation of the complex [18].

To investigate whether the interactions between SNAC and insulin affect the cellular internalization of insulin, we incubated the mixture solution with Caco-2 cells at various concentrations, ratios and pH values. The viability of cells grown in the physical mixture solution with a SNAC-to-insulin ratio of less than 80:1 reached 90%, indicating that the solution was nontoxic (Fig. S3 in Supporting information). When the FITC-Ins concentration was higher than 40 μg/mL and the ratio of SNAC to insulin was larger than 20:1, the cellular uptake amount of FITC-Ins was enhanced by approximately 3.8-fold compared with that of free insulin (pH 7.4) (Fig. 2A). Then, we fixed the concentration of insulin (50 μg/mL) to further determine the effect of pH on cellular uptake. When the pH of the mixture solution reached 6.0, there were no significant differences in cellular uptake at different ratios of the FITC-Ins and SNAC physical mixture solution, which was consistent with the above results (Fig. 2B). Confocal laser scanning microscopy (CLSM) was utilized

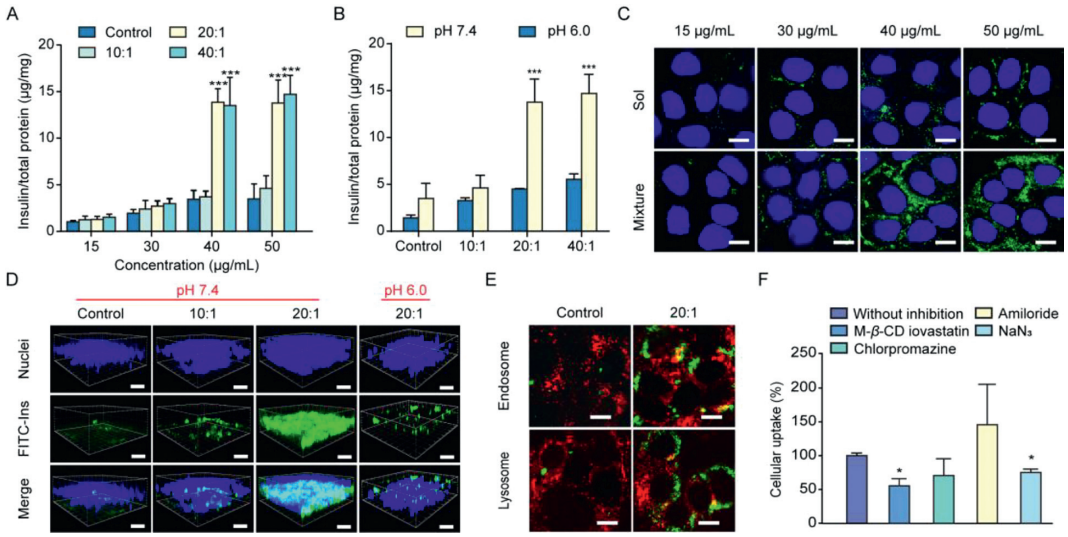

Fig. 2. *In vitro* cellular uptake analyses of physical mixture solutions. (A) Caco-2 cellular uptake of the FITC-Ins and SNAC physical mixture solution (Mixture) at different concentrations (15, 30, 40 and 50 μg/mL) and ratios (5:1, 10:1, 20:1 and 40:1, mean ± SD, $n = 3$). $^{*}P < 0.05$, $^{**}P < 0.01$, $^{***}P < 0.001$, compared with control groups. (B) Caco-2 cellular uptake of the FITC-Ins and SNAC physical mixture solution (Mixture) under different pH conditions (mean ± SD, $n = 3$). $^{*}P < 0.05$, $^{**}P < 0.01$, $^{***}P < 0.001$, compared with control groups. (C) 2D confocal microscopic images of Caco-2 cells treated with different formulations. Scale bar, 20 μm. (D) 3D confocal microscopic images of Caco-2 cells treated with different formulations under different pH conditions. Scale bar, 40 μm. (E) Colocalization images of FITC-Ins (green fluorescence) in the endosome and lysosome (red fluorescence). Scale bar, 20 μm. (F) Cellular uptake of insulin in the presence of different inhibitors (mean ± SD, $n = 3$). $^{*}P < 0.05$, compared with that without inhibition.

to observe the cellular uptake of FITC-Ins, we chose a fixed ratio (SNAC:FITC-Ins = 20:1) with different concentrations of FITC-Ins. Regardless of the concentration of FITC-Ins, the internalization of FITC-Ins into Caco-2 cells was difficult when the cells were incubated without SNAC. Stronger green fluorescence was observed when FITC-Ins at a concentration higher than 40 μg/mL was incubated with SNAC (Fig. 2C). These results strongly support our hypothesis that SNAC effectively promotes the cellular uptake of insulin when the interaction occurs at an appropriate concentration, ratio and pH.

To investigate whether SNAC changes the exocytosis rate of insulin, the intracellular distribution of FITC-Ins was observed by CLSM. We chose a fixed concentration of FITC-Ins (50 μg/mL) with different ratios of SNAC to FITC-Ins and different pH values. When the pH of the mixture solution was 7.4, most of the fluorescence signals were observed on the apical side at a ratio of 10:1. Interestingly, when the ratio reached 20:1, stronger fluorescence signals were observed by deeper scanning, indicating that most of the insulin reached the basolateral side. However, when the pH of the mixture solution was 6.0, FITC-Ins (SNAC:FITC-Ins = 20:1) was concentrated in the middle part of the cytoplasm, and formation of the complex seemed to promote the exocytosis of insulin (Fig. 2D). The semiquantitative results also confirmed our findings (Fig. S4 in Supporting information). However, when and where the complex dissociates need to be further studied.

We also utilized the E12 cell line, which can secrete mucus [19], to observe the cellular uptake of insulin and to study the effects of mucus on the uptake of the 'complex'. As shown in Fig. S5A (Supporting information), free FITC-Ins was partially located in the mucus layer, and fewer green signals were present in the cell layers when E12 cells were incubated with FITC-Ins solution. The signals of the SNAC and FITC-Ins mixture solution were stronger in the cell layer, indicating that the mucus layer barrier did not prevent SNAC from promoting insulin absorption.

The quantitative results were consistent with those obtained from CLSM. In order to distinguish the part of FITC-Ins adhered to the mucus layer, formalin solution was used to remove the mucus layer by washing the monolayers twice. Fig. S5B (Supporting information) shows that the total amount of FITC-Ins taken up by E12 cells was 1.7%. After removing the mucus layer, only 0.9% of the FITC-Ins was inside the E12 cells, indicating that nearly half of the FITC-Ins molecules were trapped in the mucus layer. The cellular uptake of the physical mixture solution was notably higher than that of the free FITC-Ins solution, reaching a maximum of approximately 5.3% FITC-Ins in the mucus layer and cells, and 3.3% were truly internalized by E12 cells. The amount of cellular uptake of the physical mixture solution was 4.4-fold more than that of the free FITC-Ins solution. Therefore, we can conclude that the formation of the complex effectively promoted insulin entry into the cells from these results.

To investigate the intracellular distribution of insulin, we determined the amounts of insulin entrapped in the endosomes and lysosomes by CLSM. As shown in Fig. 2E and Fig. S6 (Supporting information), only a few insulin molecules were captured by lysosomes and endosomes in the physical mixture solution group. The colocalization ratios of FITC-Ins with endosomes and lysosomes in the physical mixture solution group (~0.03) indicated that the 'complex' may have entered the cell through passive diffusion. To further explore whether the presence of SNAC changed the uptake pathway of insulin, we studied this pathway after the addition of various inhibitors. Fig. 2F shows that the amount of insulin taken up was reduced by approximately 24% after NaN_3 was added at 37 °C. As NaN_3 inhibits energy-dependent endocytosis, we concluded that the majority (76%) of insulin may have entered the cell through passive diffusion. The uptake amount was reduced by approximately 45% after treatment with M-1β-CD lovastatin, which indicated that caveolin-mediated endocytosis was involved in the cellular uptake of the 'complex'. These results illustrated that after the interaction between SNAC and insulin, insulin entered the cell mainly by passive diffusion and partly by active transportation.

As we found that the interaction between SNAC and insulin was concentration-, ratio- and pH-dependent, Eudragit® S100 microspheres were then designed to entrap both SNAC and insulin at a specific ratio (see synthesis details in Supporting information). As shown in Fig. 3A, the microspheres showed a clear spherical morphological appearance with a smooth surface observed by scanning

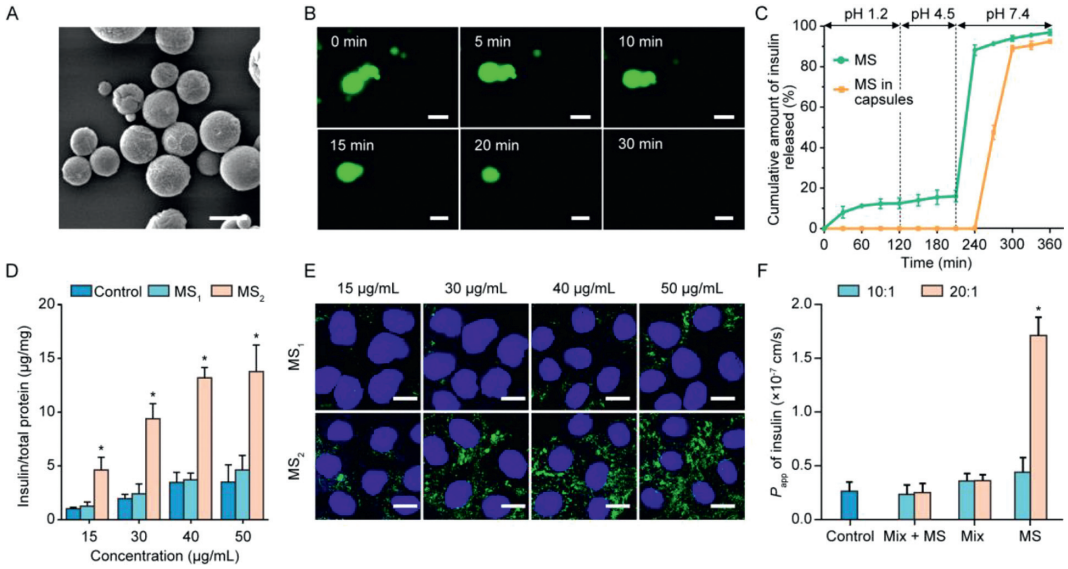

Fig. 3. Characterizations of microspheres and *in vitro* cellular uptake analyses of microspheres. (A) SEM micrographs of the microspheres. Scale bar, 10 μm. (B) Micrographs of the microspheres in pH 7.4 media after incubation for 30 min. Scale bar, 10 μm. (C) Release profiles of insulin from the microspheres (MS) and enteric-coated capsules in diverse pH environments. (D) Cellular uptake of insulin from different microspheres (mean ± SD, $n = 3$). $^*P < 0.05$, compared with control groups. (E) 2D confocal microscope images of Caco-2 cells treated with different formulations. Scale bar, 40 μm. (F) P_{app} of insulin from different formulations (FITC-Ins: 15 μg/mL) across Caco-2 cell monolayers (mean ± SD, $n = 3$). $^*P < 0.05$, compared with MS_1.

electron microscopy (SEM). The mean particle size of the microspheres was 10.1 ± 2 μm (Fig. S7 in Supporting information).

The dissolution of the microspheres incubated at pH 7.4 was observed by fluorescence microscopy. As shown in Fig. 3B, the microspheres almost maintained their original shapes in the first 5 min. The particle size of the microspheres gradually decreased over the next 10 min, indicating that the microspheres began to dissolve. The microspheres were completely dissolved within 30 min.

To prevent the enzymatic degradation and release of insulin in the stomach and the upper small intestine, the microspheres were loaded into Eudragit® S100-coated capsules for colon-targeted delivery [20]. Eudragit® S100 is an anionic copolymer comprised of methacrylic acid and acrylates that dissolves at pH > 7.0 [21]. The release characteristics of insulin released from the microspheres and the enteric-coated capsules *in vitro* are shown in Fig. 3C. The microspheres released approximately 18% of the insulin at pH 1.2 and 4.5, which may have contributed to the release of insulin attached to the surface of the microspheres. At pH 7.4, the microspheres became unstable, leading to the rapid release of insulin. For the microspheres loaded into the Eudragit® S100-coated capsule, we did not notice any release of insulin until the pH reached 7.4, indicating that the preparation could protect insulin against gastric degradation. Further, it can slowly release its drug load in the colon at pH 7.4. The circular dichroism (CD) results indicated that the structure of the released insulin was not destroyed (Fig. S8 in Supporting information).

We prepared two types of microspheres with SNAC:FITC-Ins ratios of 10:1 (MS_1) and 20:1 (MS_2). Fig. S9 (Supporting information) shows the fluorescence intensity of FITC-Ins released from the two types of microspheres. MS_1 was unable to reduce the fluorescence intensity regardless of the concentration. However, the fluorescence intensity of MS_2 was markedly reduced to 78% when the concentration of FITC-Ins was 50 μg/mL, indicating that an interaction occurred between SNAC and insulin. Interestingly, after encapsulating SNAC and FITC-Ins into MS_2, the fluorescence intensity was reduced even at 15 μg/mL. This phenomenon might be attributed to the high local concentration caused by the microspheres.

Caco-2 cellular uptake experiments also demonstrated that the cellular uptake amount of insulin released from MS_2 was higher than that released from MS_1 by almost 3.1–4.4 folds (Fig. 3D). Caco-2 cellular uptake of FITC-Ins from the microspheres visualized by CLSM also strongly supported the findings of the quantitative studies. Stronger green fluorescence was detected when Caco-2 cells were incubated with MS_2 (Fig. 3E). For MS_1, the fluorescence intensity observed for different concentrations of FITC-Ins was almost nondetectable, which was potentially due to the lack of interaction between SNAC and insulin. Likewise, as shown in Fig. 3F, the apparent permeability coefficient (P_{app}) value of insulin from MS_2 was 5.2 times higher than that of the blank microspheres with physical mixture solution (Mix + MS) and 3.3-fold higher than that of MS_1 (the concentration of FITC-ins in all of these preparations is 15 μg/mL). This result further confirmed our previous finding that SNAC promoted the transepithelial transport of insulin. SNAC has been reported to change the transepithelial electrical resistance (TEER) value at a high concentration [22]. The concentrations of SNAC we used in this study (up to 300 μg/mL) did not affect the TEER, suggesting that the improved permeation of insulin was not caused by the alteration of epithelial membrane integrity or tight junction opening (Fig. S10 in Supporting information). This might have been due to the interaction between SNAC and insulin based on growing lipophilicity through hydrogen bonding and/or hydrophilic interactions. We also confirmed that MS_2 was safe at the tested concentrations (3, 9 and 15 mg/mL, Fig. S11 in Supporting information). These results verified that microspheres with a ratio of 20:1 lowered the concentration threshold of the interaction between SNAC and insulin and effectively improved the cellular uptake and transepithelial transport of insulin.

Next, we evaluated the intestinal absorption of the different capsules *in vivo*. All of the animal experiments were performed in compliance with the Institutional Animal Care and Use Committee (IACUC) guidelines of Shanghai Institute of Materia Medica (IACUC code: 2020–05-GY-58). As shown in Fig. 4A and Fig. S12 (Supporting information), Eudragit® S100-coated capsules filled with

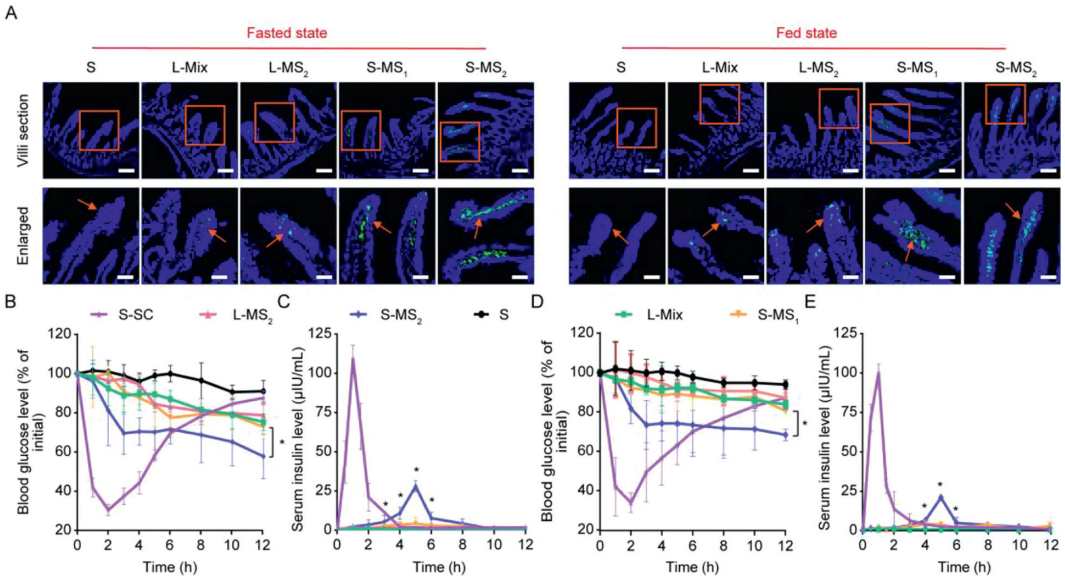

Fig. 4. *In vivo* intestinal villus absorption of insulin-loaded capsules and pharmacodynamic and pharmacokinetic studies of insulin-loaded capsules. (A) Intestinal absorption of insulin in fasting rats and in rats fed freely. (Up) Scale bar, 100 μm. (Down) Scale bar, 50 μm. Blood glucose levels of the diabetic rats following the oral administration of insulin-loaded capsules or an insulin solution (S, 30 IU/kg) or the subcutaneous injection of the insulin solution (S-SC, 5.0 IU/kg) in fasting rats (B) and in rats fed freely (D). Serum insulin levels of the diabetic rats following administration of the same formulations in fasting rats (C) and in rats fed freely (E) (mean ± SD, $n = 3$). $^{*}P < 0.05$, compared with S-MS_1.

MS_2 (S-MS_2) seemed to have better absorption properties than the others. Eudragit® L100-coated capsules filled with MS_2 (L-MS_2) did not show such remarkable characteristics due to the pH effect. Eudragit® S100-coated capsules filled with MS_1 (S-MS_1) and Eudragit® L100-coated capsules filled with mixture powder (L-Mix) also showed limited absorption due to no complex formation. It is noteworthy that the final concentration of FITC-ins in all of these preparations is 15 μg/mL. Surprisingly, the same trend was shown in the rats fed freely, indicating that food hardly affected insulin absorption in S-MS_2 we designed.

To further evaluate the effect of the interaction between SNAC and insulin on absorption, a two-photon microscope was used to observe the real-time absorption of insulin released from S-MS_1 and S-MS_2 in rat intestinal villi. A great quantity of insulin released from S-MS_2 was transported into the intestinal villi and absorbed by cells over time compared with that of S-MS_1. The presence of food did not affect the absorption of the complex to a large extent (Fig. S13 in Supporting information and Movies S1-S4 in Supporting information).

Finally, we evaluated the hypoglycemic effect and the serum insulin level in diabetic rats administrated various capsules orally. In diabetic rats, oral administration of a free insulin solution had almost no significant blood sugar lowering effect due to the degradation by gastric and proteases *in vivo*. Surprisingly, the oral administration of S-MS_2 showed a significant hypoglycemic effect, with a maximal blood glucose reduction of 55% and no risk of hypoglycemia (Fig. 4B and Fig. S14 in Supporting information). The pharmacological availability (PA%) of S-MS_2 was 13.2%, which was 8.2 times higher than that of free insulin (Table S1 in Supporting information). A nonsignificant decrease in blood glucose levels observed with S-MS_1 may have been attributed to the lack of interaction between SNAC and insulin; thus, SNAC may not promote oral insulin absorption. These results were consistent with our findings from cellular studies. Interestingly, the hypoglycemia effect of Eudragit® L100-coated capsule was less remarkable than that resulting from oral administration of the Eudragit® S100-coated capsule, which could be explained by two reasons: (1) Eudragit® L100 dissolved at pH > 5.5 [23], and SNAC and insulin could not interact at such a low pH; (2) the insulin released from the capsules was potentially degraded by the proteases in the upper small intestine. Moreover, the blood glucose level did not recur to the baseline after 10 h. In addition, in the rats fed freely, S-MS_2 exhibited the most remarkable hypoglycemic effect, with a PA% of 12.1%, which suggested that food didn't affect its efficacy (Fig. 4D and Table S2 in Supporting information).

The serum insulin concentration-time profiles are shown in Figs. 4C and E, respectively. The rats subcutaneously (SC) injected with the free insulin solution showed the maximal serum insulin concentration at 1 h after administration. In fasting rats, the oral administration of S-MS_2 generated a slower but prolonged increase in the serum insulin concentration, and the concentration peaked at 5 h, yielding a relative bioavailability of 6.3%, which was 3.3 times higher than that of S-MS_1. In contrast, a negligible amount of plasma insulin was found in the rats orally administrated L-mixture or L-MS_2 (Table S1). To our surprise, the rats fed freely taking S-MS_2 orally had a relative bioavailability of 6.3%, which was consistent with that of the fasting rats (Table S2). These results showed that the preparation we designed prevents the influence of food and has a significant hypoglycemic effect.

In this study, we found that SNAC could adhere to insulin in a specific concentration-, ratio- and pH-dependent manner. *In vitro* studies demonstrated that the interaction between SNAC and insulin improved the cellular uptake and enhanced the intestinal mucosal permeability of insulin. Based on this finding, Eudragit® S100 microspheres were designed to entrap both SNAC and insulin at a specific ratio. The *in vivo* study results also showed that the oral administration of the specific microsphere-loaded Eudragit® S100-coated capsules exhibited an approximately 6.3% oral bioavailability in diabetic rats in both the fasted and fed states. In summary, we successfully constructed an SNAC-based oral insulin delivery system that has high oral bioavailability and patient-friendly medication guidance, which might pave the way for the rational design of oral macromolecule formulations.

Declaration of competing interest

The authors report no declarations of interest.

Acknowledgments

The authors are grateful for the financial support from the National Natural Science Foundation of China (Nos. 81773651, 82025032 and 82073773), NN-CAS foundation, National Key R&D Program of China (No. 2020YFE0201700), Chinese Pharmacopoeia Commission (Nos. 2021Y30 and 2021Y25), the Shanghai Science and Technology Committee (No. 18430721600) and the Major International Joint Research Project of Chinese Academy of Sciences (No. 153631KYSB20190020). We also thank Dr. Zhuo Li from NanoTemper Technologies for performing the MST measurement and data analysis.

Supplementary materials

Supplementary material associated with this article can be found, in the online version, at doi:10.1016/j.cclet.2021.10.023.

References

[1] D.J. Drucker, Nat. Rev. Drug Discov. 19 (2019) 1–13.
[2] C. Hu, W. Jia, Adv. Drug Deliv. Rev. 139 (2019) 3–15.
[3] Y. Han, Z. Gao, L. Chen, et al., Acta Pharm. Sin. B 9 (2019) 902–922.
[4] M. Sun, H.K. Hu, L.M. Sun, et al., Chin. Chem. Lett. 31 (2020) 1729–1736.
[5] J. Qi, J. Zhuang, Y. Lv, Y. Lu, W. Wu, J. Control. Release 275 (2018) 92–106.
[6] Y.L. Bai, R. Zhou, L. Wu, et al., J. Mat. Chem. B 8 (2020) 2636–2649.
[7] S. Maher, R.J. Mrsny, D.J. Brayden, Adv. Drug Deliv. Rev. 106 (2016) 277–319.
[8] V. Gupta, B.H. Hwang, N. Doshi, S. Mitragotri, J. Control. Release 172 (2013) 541–549.
[9] C. Twarog, S. Fattah, J. Heade, et al., Pharmaceutics 11 (2019) 78.
[10] S. Maher, D.J. Brayden, L. Casettari, L. Illum, Pharmaceutics 11 (2019) 41.
[11] S. Maher, C. Geoghegan, D.J. Brayden, Expert Opin. Drug Deliv. 18 (2020) 273–300.
[12] D.J. Brayden, J.P. Gleeson, E.G. Walsh, Eur. J. Pharm. Biopharm. 88 (2014) 830–839.
[13] D. Malkov, R. Angelo, H.Z. Wang, et al., Curr. Drug Deliv. 2 (2005) 191–197.
[14] D. Malkov, H.Z. Wang, S. Dinh, I. Gomez-Orellana, Pharm. Res. 19 (2002) 1180–1184.
[15] C. Granhall, M. Donsmark, T.M. Blicher, et al., Clin. Pharmacokinet. 58 (2019) 781–791.
[16] M. Kidron, S. Dinh, Y. Menachem, et al., Diabet. Med. 21 (2004) 354–357.
[17] R. Eldor, E. Arbit, A. Corcos, M. Kidron, PLoS One 8 (2013) e59524.
[18] R.A. Ogg, O.K. Rice, J. Chem. Phys. 5 (1937) 140–143.
[19] M. Liu, J. Zhang, X. Zhu, et al., J. Control. Release 222 (2016) 67–77.
[20] S. Chen, F. Guo, T. Deng, et al., AAPS PharmSciTech 18 (2017) 1277–1287.
[21] D. Jain, A.K. Panda, D.K. Majumdar, AAPS PharmSciTech 6 (2005) E100–E107.
[22] D. Brayden, E. Creed, A. O'Connell, et al., Pharm. Res. 14 (1997) 1772–1779.
[23] D. Jain, D.K. Majumdar, A.K. Panda, J. Biomater. Appl. 21 (2006) 195–211.